ISSN: 0067-2904

Shell model study of neutron rich $^{18-28}$O isotopes using effective interactions

Adel K. Hamoudi, Hussam A. Bahr*
Department of Physics, College of Science, University of Baghdad, Baghdad, Iraq.

Abstract

We employ a simple effective nucleon-nucleon interaction for sd-shell model calculations derived from the Reid soft-core potential folded with two-body correlation functions which take account of the strong short-range repulsion and large tensor component in the Reid force. Shell model calculations for ground and low lying energy states of neutron rich oxygen isotopes $^{18-28}$O are performed using OXBASH code. Generally, this interaction predicts correct ordering of levels, yields reasonable energies for ground states of considered isotopes and predicts very well the newly observed excitation energy of 2_1^+ $(1.28^{+0.11}_{-0.08})$ in ^{26}O. Besides, it produces reasonable energy spectra for $^{23-27}$O and compressed energy spectra for $^{18-22}$O isotopes. This is mainly due entirely to defects in the $T = 1$ diagonal matrix elements of employed interaction. To improve the present calculations, we modify the interaction through replacing the 14 diagonal matrix elements of $T = 1$ with those of the USD interaction. Mostly, our modified interaction predicts well the ordering of levels, the ground state energies and low lying energy spectra for all selected oxygen isotopes. The modified interaction confirms the location of the neutron drip line at $N = 16$ and also identifies the presence of the shell gap at $N = 14$ and $N = 16$, which proves the doubly magic behavior of ^{22}O and ^{24}O. The spins in ^{24}O of several excitation energies around 7.5 MeV are predicted by our interactions. The calculated results obtained with the modified interaction are very close to those obtained with the empirical interactions of USDB and WPN.

Keywords: energy spectrum, energy levels, binding energy, oxygen isotopes, shell model.

دراسة أنموذج القشرة لنظائر الاوكسجين $^{18-28}$O الغنية بالنيوترونات بأستخدام تفاعلات مؤثرة

عادل خلف حمودي ، حسام علي بحر*
قسم الفيزياء ، كلية العلوم ، جامعة بغداد ، بغداد ، العراق

الخلاصة

تم استخدم تفاعل مؤثر بسيط للنيوكليون– نيوكليون في حسابات أنموذج القشرة sd المشتق من جهد Ried مع دالة الربط للجسيمتين التي تأخذ بنظر الاعتبار التنافر القوي عند المدى القصير ومركبة Tenser

*Email: hussan_aba90@yahoo.com

الطويلة في قوة Ried. حسابات أنموذج القشرة للحالات الارضية والمتهيجة الواطئة لنظائر الاوكسجين $^{18-28}$O الغنية بالنيوترونات أجريت بأستخدام البرنامج OXBASH. عموما" هذا التفاعل يتوقع تسلسل صحيح للمستويات ويعطي تطابق مقبول لطاقات الحالات الارضية للنظائر قيد الدراسة. وكذلك يتوقع تطابق ممتاز لمستوى الطاقة $(1.28^{+0.11}_{-0.08})$ 2^+_1 المكتشف حديثا" في نواة ^{26}O. الى جانب ذلك هذا التفاعل حقق تطابق مقبول لأطياف الطاقة بالنسبة للنظائر $^{23-27}$O ومظغوط نسبيا" للنظائر $^{18-22}$O. ان سبب ذلك يعود الى عيوب في العناصر القطرية التي لها T=1 لمصفوفة هذا التفاعل. ولتحسين الحسابات تم تعديل هذا التفاعل من خلال استبدال العناصر القطرية لمصفوفة التفاعل (لها T=1) مع تلك الموجودة بتفاعل USD. غالبا التفاعل المعدل يتوقع تسلسلات جيدة للمستويات وكذاك يتوقع نتائج جيدة لطاقات الحالات الارضية والمتهيجة الواطئة لكل نظائر الاوكسجين قيد الدراسة. ان التفاعل المعدل يؤكد بأن خط تقطير النيوترونات عند N=16 وكذلك اثبت بأنه هنالك فجوة للقشرة النووية عند N=14 و N=16 والتي تؤيد بأن النوى ^{22}O و ^{24}O هي نوى سحرية مضاعفة. الزخم الزواي للحالات المتهيجة القريبة من الطاقة 7.5 MeV تم حسابها بأستخدام التفاعلان المعدل والغير معدل.

Introduction

The nuclear shell model is the basis on which our understanding of nuclei is built. Today, one of the most significant difficulties in nuclear structure is to realize how shell structure varies with neutron-to proton ratio in the nuclear chart. Shell structure effects on positions of the neutron and proton drip lines and the stability of atomic nuclei. An essential feature of the shell structures in all nuclei is the existence of gaps in the single-particle spectra. The magic numbers 2, 8, 20, 28, 50, 82, and 126 connected with the filling of the nucleon orbitals up to the shell gaps in nuclei near stability are well established [1]. For nuclei away from stability the shell gaps can change as in ^{22}O and ^{24}O isotopes. Neutron-rich oxygen isotopes are essentially exciting nuclei because of the following reasons: First, the nuclei ^{22}O and ^{24}O reveal double magic property at the neutron numbers $N = 14$ and $N = 16$, respectively [2–4]. Second, oxygen is the densest element for which the neutron drip line is recognized experimentally. The latest experimental investigations [5, 6] demonstrate obviously that the nuclei ^{25}O and ^{26}O are unbound, consequently making ^{24}O the most neutron-rich bound isotope of oxygen. The spectroscopy of the drip line nucleus ^{24}O was investigated in the experiment [7]. One of the significant results of this investigation is a state with an unidentified spin and parity at approximately 7.5 MeV of excitation energy. Theoretical researches in this area of the nuclear chart are challenging [8–10]. Volya and Zelevinsky [8] utilized an empirical two-body interaction (above the core of ^{16}O) and involved the particle continuum in their shell model evaluation of neutron-rich oxygen isotopes. Otsuka et al. [10] involved three-nucleon forces (3NFs) through the sd-shell model (taking ^{16}O as an inert core with empirical single-particle energies) and noticed that three-body forces produce ^{24}O at the neutron drip line. The ab initio calculations of neutron-rich oxygen isotopes by Hagen et al. [9] used microscopic interactions from chiral effective field theory [11], had no core, but were limited to nucleon-nucleon (NN) interactions.

In the present work, a simple effective nucleon-nucleon interaction [12] for sd-shell model calculations is used. This interaction (denoted by I_1) was derived from the Reid soft-core potential [13] folded with two-body correlation functions which take account of the strong short-range repulsion and large tensor component in the Reid force. In general, I_1 interaction expects right sequence of energy levels, provides reasonable energies for ground states of considered nuclei and predicts very well the recently observed excitation energy of 2^+_1 in ^{26}O. Also, it produces reasonable energy spectra for $^{23\text{-}27}$O isotopes and compressed energy spectra for $^{18\text{-}22}$O isotopes. This is essentially attributed to the weakness of the $T = 1$ diagonal matrix elements of our I_1 interaction. To improve the calculations, the interaction I_1 is modified through replacing the 14 diagonal matrix elements of $T = 1$ with those of the USD interaction [14]. The predicted properties with this modified interaction (denoted by I_2) for new magic nuclei that have been observed in the neutron-rich oxygen isotopes ($Z = 8$) out to the neutron drip line at neutron number $N = 16$ are discussed. Furthermore, the spins in ^{24}O of several excitation energies around 7.5 MeV are predicted and consequently shed light on the

experiment [7]. It is found that the calculated results achieved with our I_2 interaction, which are in very good agreement with experiment, are very close to those obtained with the empirical interactions of WPN [14] and USDB [15].

Formalism

Our method [12] to the problem of effective operators for shell model calculations included two steps. In the first step the bare operator must be expressed in the rest frame of the nucleus and can be formulated as

$$\hat{H} = \sum_{i>j} \left[\frac{p_{ij}^2}{M(A)} + V_{ij} \right], \quad (1)$$

where $p_{ij} = (1/\sqrt{2})(p_i - p_j)$ is the relative momentum, $M(A) \simeq Am_N$ is the total mass of the nucleus (m_N is mass of the neutron) and V_{ij} is chosen to be the Reid soft-core potential. The second step is to consider a set of trial variational wave functions

$$\Psi_J = F\Phi_J, \quad (2)$$

where Φ_J are the usual shell model basis states and F is a correlation function designed to accommodate those correlations which cannot be described by the shell model configuration mixing. A complete set of effective shell model operators is then defined by [16]

$$O_{eff} = F^+ \hat{O} F \quad (3)$$

This in fact is a many-body operator and it would be extremely unreasonable to work therefore it is customary to make a cluster expansion of O_{eff} to get a set of two body effective operators $O_{eff}^{(2)}$. In the case of the operator of eq. (1) [12]

$$H_{eff}^{(2)} = F_2^+ \hat{H} F_2 \equiv \sum_{i>j} f_{ij}^{\lambda} \left(\frac{p_{ij}^2}{M(A)} + V_{ij} \right) f_{ij}^{\lambda}, \quad (4)$$

where $F_2 = f_{ij}^{\lambda}$ are two body correlation operators and λ is summed over two body channels.

From the analysis of the nuclear matter saturation problem [16] it is obvious that the correlation operators have to take two features into account:

(a) The short-range exclusion effect formed by the repulsive core of the bare N-N interaction. The core has a very short range (~ 0.4 fm) and the wound that it initiates in the nuclear wave function is a property of the potential rather than the specific environment that the nucleon finds itself in. Therefore, if f_{ij}^{λ} is limited to characterizing this short-range effect, leaving the shell model configuration mixing to account for longer-range correlations, two advantages can be gained. Being short ranged, any cluster expansion will rapidly converge and the two-body approximation for $H_{eff}^{(2)}$ of eq. (4) can be justified. Moreover, the wound will be independent of mass, i.e. of the nucleus being considered.

(b) The strong correlations initiated by the tensor force component in V_{ij}. These correlations are of longer range and may be expected to reveal mass dependence.

Irvine et al. [17] introduced the simple parameterization

$$f_{ij}^{\lambda} = f(r_{ij})(1 + \alpha^{\lambda}(A) S_{ij}), \quad (5)$$

where $f(r_{ij})$ has the form

$$f(r_{ij}) = 1 - exp\left[-\beta (r_{ij} - r_c)^2 \right], \quad (6)$$

with $r_c = 0.25$ fm and $\beta = 25$ fm^{-2}, and represents the short-range repulsion of (a). S_{ij} is the usual tensor operator and the strength of tensor correlations of (b) is measured by $\alpha^{\lambda}(A)$, where $\alpha^{\lambda}(A) \equiv 0$ for $\lambda \neq {}^3S_1$-$^3D_1$. We shall hereafter drop the label λ. The magnitude of $\alpha(A)$ was determined [16] by fitting it to the ground state binding energies of ^{4}He and ^{16}O calculated in the closed shell approximation with oscillator wave functions chosen to give the correct root mean square radii, and to a Hartree-Fock calculation for nuclear matter. The result was a monotonically decreasing function with $\alpha(4) = 0.1$, $\alpha(16) = 0.08$ and $\alpha(\infty) = 0.06$. In the p-shell analysis the interpolation between

$A = 4$ and $A = 16$ was made by fitting the ground state binding energy of the most stable isobar for each value of A.

The traditional method to the nuclear shell model is to select a single-particle basis and separate it into an inert set of core states and active valence states. The core states basically donate a constant E_0 to the absolute binding energy and the relative energy spectrum is established by diagonalizing the Hamiltonian matrix [12]

$$H_{IJ} \equiv E_0 + \sum_{i \in I(v)} \varepsilon_i \, \delta_{IJ} + \sum_{\substack{i>j \in I(v) \\ k>l \in J(v)}} \langle ij|V|kl\rangle \, \delta(I - ij; J - kl), \qquad (7)$$

with

$$\varepsilon_i = \sum_{a \in core} \langle ai|V|ai\rangle, \qquad (8)$$

where the representation is that $I(v)$ and $J(v)$ are shell model configurations of active nucleons in the valence space and the $\delta(I - ij; J - kl)$ assists to remind us that with a two-body interaction the configuration I can differ from J at most by the movement of two-particles. In eq. (7) only valence orbit labels are summed over.

Results and discussion

The elementary input to a nuclear shell model calculation consists of a set of single particle energies and two body interaction matrix elements (2bme's). The 2bme's for sd-shell nuclei consist of 63 matrix elements with 28 diagonals (14 with $T = 0$ and 14 with $T = 1$) and 35 off-diagonal (19 with $T = 0$ and 16 with $T = 1$). Shell model calculations for neutron rich $^{18\text{-}28}$O nuclei in the sd-shell are performed using OXBASH code [18]. Our interaction 2bme's of I_1 and I_2 designated for the sd-shell nuclei are used in the present calculations together with the empirical single-particle energies of the USD interaction [14], namely: -3.9477999, -3.1635399 and 1.6465800 MeV for $j = 5/2, 1/2$ and $3/2$, respectively. The sd-shell neutron rich oxygen isotopes are assumed to have an inert closed shell core of ^{16}O and (A-16) outer valence neutrons move in the $0d_{5/2}$, $1s_{1/2}$ and $0d_{3/2}$ orbitals. The orbitals are labeled by (n, l, j), where n is the number of times the radial wave function crosses zero, l is the orbital angular momentum, and j is the total (orbital plus spin) angular momen

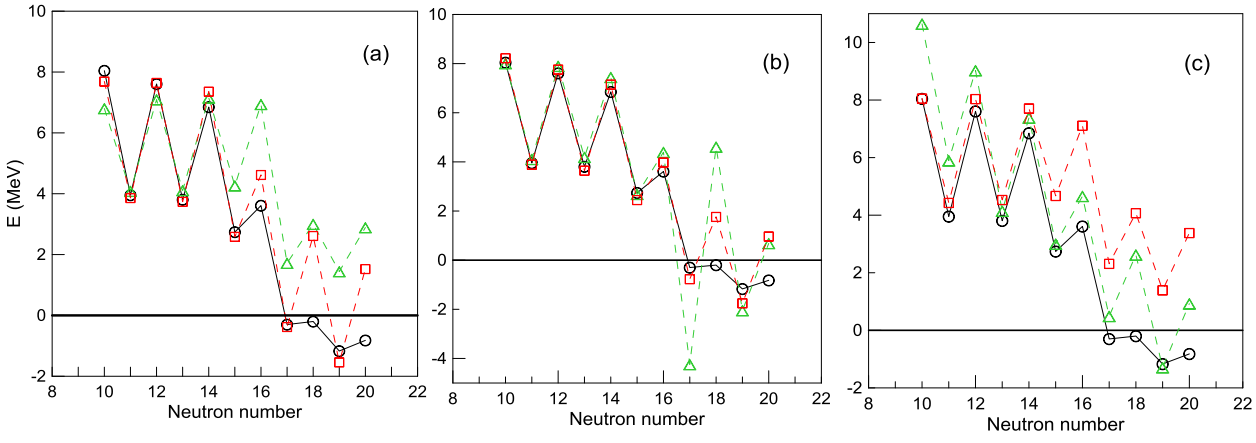

Figure 1- Single neutron separation energies for the oxygen isotopes as a function of the neutron number. Black circles are the experimental values taken from [19]. Green triangles and Red squares are, correspondingly, those obtained with: (**a)** our I_1 and I_2, **(b)** USDB and WPN, and **(c)** MSDI and KUOSD interactions.

Figure-1 displays the single neutron separation energies for the oxygen isotopes (the smallest amount of energy needed to liberate one neutron). The experimental values [19], displayed as black circles, exhibit the usual odd-even fluctuation related with the pairing interaction between neutrons. It

is evident from the experimental values that the nucleus with $N = 16$ is the last bound nuclei in neutron-rich side of oxygen isotopes. Away from $N = 16$ the nuclei are outside the drip line (i.e., unbound nuclei) and the neutron separation energy is sudden drop from a positive value for $N = 16$ to a negative value for $17 \leq N \leq 20$. The experimental values for the neutron separation energy are compared with those of our I_1 [12] and present modified I_2 interactions (Figure-1(a)), empirical interactions of WPN [14] and USDB [15] (Figure-1(b)) and theoretical interactions of MSDI [20] and KUOSD [21] (Figure-1(c)). The predicted results of our I_1 interaction (denoted by green triangles) fail to reproduce the drip line at $N = 16$ and also fail to give a negative value for $17 \leq N \leq 20$. However, an improved result can be obtained when we modify I_1 interaction via replacing the 14 diagonal matrix elements of $T = 1$ with those of the USD interaction [14]. The results of this I_2 interaction (denoted by red squares) show a good agreement with experiment.

Besides, the neutron drip line is now located at $N = 16$ in agreement with experiment. The discrepancies in I_1 interaction [12] are then due entirely to defects in the diagonal $T = 1$ matrix elements. In Figure-1(b), the agreement with experiment is good for WPN and USDB with the neutron drip line at $N = 16$. In Figure-1(c), the drip line is extended to $N = 18$ (with the MSDI) and $N = 20$ (with the KUOSD), which is in disagreement with experiment. It is so clear from this figure that our improved interaction (red squares in Figure-1(a)) gives results very close to those of empirical interactions Figure-1(b).

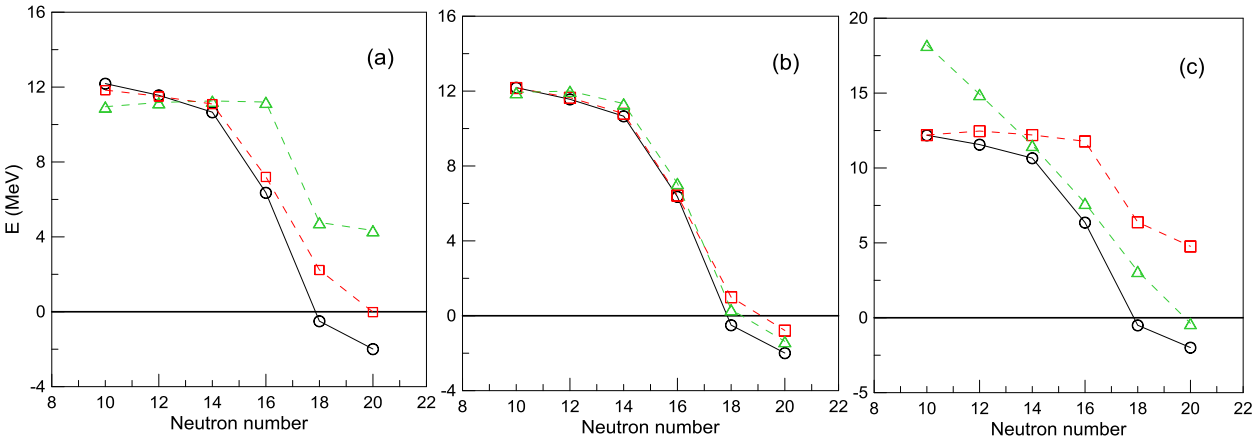

Figure 2- Two neutron separation energies for the oxygen isotopes as a function of the neutron number. Black circles are the experimental values taken from [19]. Green triangles and Red squares are, correspondingly, those obtained with: **(a**) our I_1 and I_2, **(b)** USDB and WPN, and **(c)** MSDI and KUOSD interactions.

Figure-2 demonstrates the two neutron separation energies for the oxygen isotopes (the minimum amount of energy required to release two neutrons). The experimental values [19], displayed as black circles, give the evidence that both ^{26}O and ^{28}O are unbound by 0.5 and 1.99 MeV, respectively. In Figure-2(a), our I_1 interaction predicts both ^{26}O and ^{28}O to be bound by 4.772 and 4.342 MeV, respectively (which is in disagreement with experiment) while our I_2 interaction predicts ^{26}O to be bound by 2.237 MeV (which is in disagreement with experiment) and ^{28}O to be unbound by 0.013 MeV (which is in agreement with experiment). In Figure-2(b), ^{26}O is found to be bound by 0.366 MeV (with the USDB) and by 0.995 MeV (with the WPN), in disagreement with experiment, while ^{28}O is found to be unbound by 1.366 MeV (with the USDB) and by 0.785 MeV (with the WPN), in agreement with experiment. In Figure-2(c), MSDI predicts ^{26}O to be bound by 3.111 MeV, in disagreement with experiment, and ^{28}O to be unbound by 0.367 MeV, in agreement with experiment while KUOSD predicts both ^{26}O and ^{28}O to be bound by 6.385 and 4.770 MeV, respectively, which is

in disagreement with experiment. It is obvious from Figure-2 that our I_2 interaction predicts nearly similar results for ^{26}O and ^{28}O as those of USDB and WPN interactions. It also offers results for oxygen isotopes better than those of MSDI and KUOSD interactions.

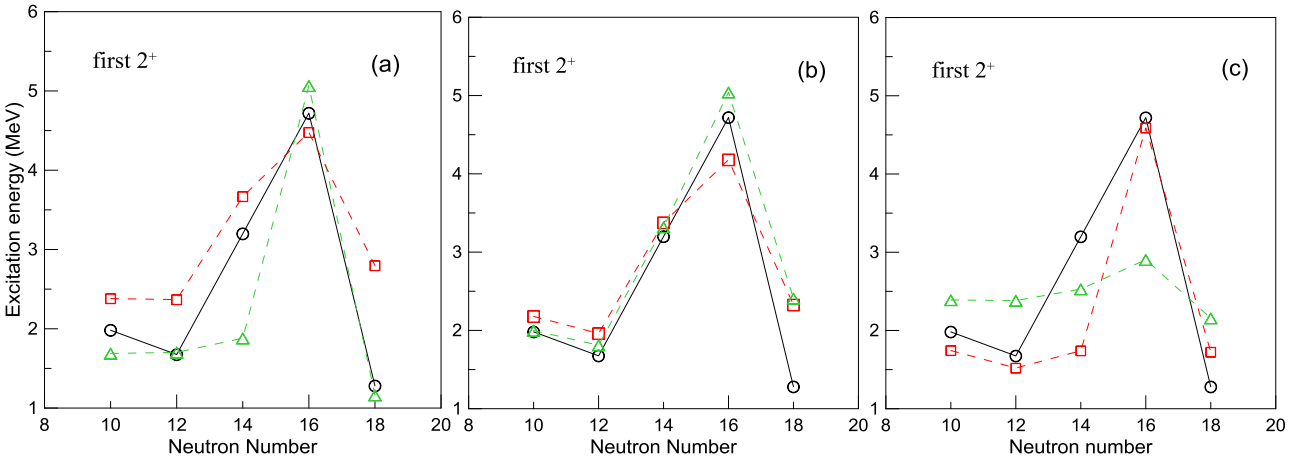

Figure 3- Excitation energy of first-excited 2_1^+ states in even-even neutron rich oxygen isotopes. Black circles are the experimental values of ^{18}O [22], ^{20}O [23], ^{22}O [23] ^{24}O [3] and ^{26}O [24]. Green triangles and Red squares are, correspondingly, those obtained with: **(a)** our I_1 and I_2 **,(b)** USDB and WPN, and **(c)** MSDI and KUOSD interactions.

Figure-3 reveals the excitation energy for the first-excited 2_1^+ states in even-even neutron rich oxygen isotopes. In Figures-3(a), 3(b) and 3(c), the experimental excitation energy of 2_1^+ states in ^{18}O [22], ^{20}O [23], ^{22}O [23], ^{24}O [3] and ^{26}O [24] (displayed as black circles) are compared with those obtained via (I_1 and I_2) interactions, empirical interactions (USDB and WPN), and theoretical interactions (MSDI and KUOSD), respectively. It is known from experiment that the excitation energy of the first-excited 2_1^+ state in even-even nuclei suddenly increases at the magic number. This property gives a strong indicator for the magic number. The doubly magic behavior of ^{22}O was first specified by the National Superconducting Cyclotron Laboratory at Michigan State University [24] where the 2_1^+ state was detected at 3.199 MeV, which is nearly twice that in the neighboring $N = 10$ and 12 nuclei, specifying the existence of the shell gap at $N = 14$. It is evident from this figure that our I_2 interaction (red squares in Figure-3(a)) and empirical interactions of USDB and WPN (Figure-3(b)) identify the presence of the shell gap at $N = 14$ and then prove the doubly magic behavior of ^{22}O. Our I_1 interaction (green triangles in Figure-3(a)) and the theoretical interactions of MSDI and KUOSD (Figure-3(c)) fail to classify the shell gap at $N = 14$ and consequently fail to describe the doubly magic behavior of ^{22}O. The nonappearance of any excited states that are bound to γ decay for ^{24}O detected in experiments at GANIL [23] suggest that its first excited state lies above the neutron separation energy of 3.6 ± 0.3 MeV. In general, the nucleus of ^{24}O has exciting properties because it lies on the neutron drip line and it has quite large neutron separation energy. The lower limit of 3.6 MeV for a bound excited state indicates a doubly magic property. The excitation energies for the 2_1^+ states are 5.066 MeV (with I_1 interaction), 4.477 MeV (with I_2 interaction), 5.042 MeV (with USDB interaction), 4.180 MeV (with WPN interaction) and 4.589 MeV (with KUOSD interaction). These excitation energies are, in agreement with experiment, above the neutron separation energy of ^{24}O, which indicate a doubly magic nature of ^{24}O. As the excitation energy for 2_1^+ state obtained with MSDI interaction (2.157 MeV) lies below the neutron separation energy of ^{24}O, the MSDI interaction fails to classify the doubly magic property of ^{24}O. Review to Figure-3 shows that our I_2 interaction provides nearly the same result as those of USDB and WPN interaction. Moreover, it also provides results for all nuclei under study better than those of MSDI and KUOSDI interactions.

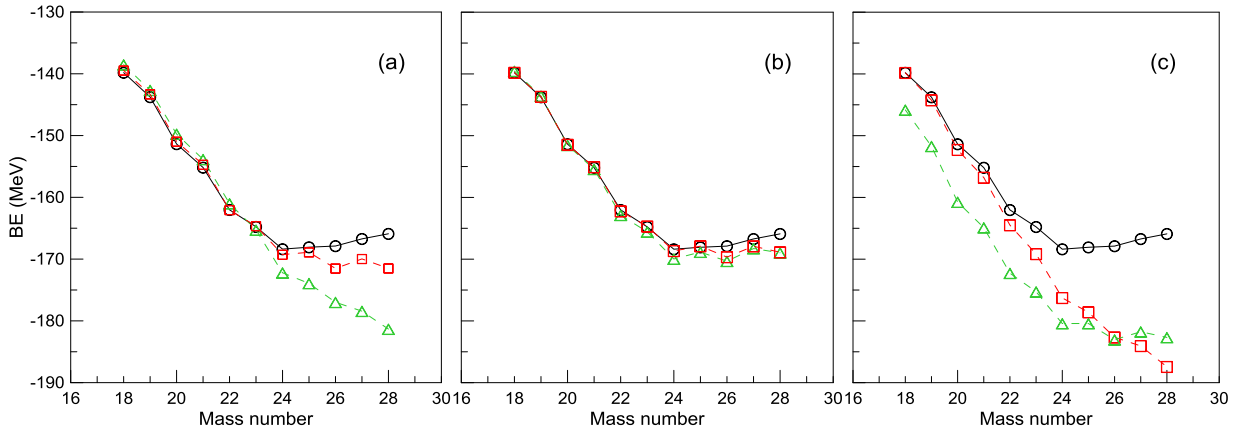

Figure 4- Ground-state binding energy of the oxygen isotopes as a function of the mass number. Black circles are the experimental values taken from [19]. Green triangles and Red squares are, correspondingly, those obtained with: **(a)** our $I_1$and I_2, **(b)** USDB and WPN, and **(c)** MSDI and KUOSD interactions.

Figure- 4 shows the ground-state binding energies for the neutron rich oxygen isotopes $^{18-28}$O. The experimental values [19] (denoted by black circles) are compared with those of our I_1 and I_2 interactions Figure-4(a), empirical interactions of USDB and WPN (Figure-4(b)) and theoretical interactions of MSDI and KUOSD (Figure- 4(c)). Our predicted results Figure- 4(a) obtained with our I_1 interaction are in agreement with the data at $18 \leq A \leq 23$ and in disagreement with the data at $24 \leq A \leq 28$ while those predicted with our I_2 interaction are in very well agreement with the data at $18 \leq A \leq 25$ and in reasonable agreement with the data at $26 \leq A \leq 28$. Moreover, the deviation between our predicted ground-state binding energies for oxygen isotopes $^{18-28}$O and those of the experimental data is noticeably reduced in the calculations of the I_2 interaction as compared with those of I_1 interaction. The computed results by USDB and WPN interactions Figure- 4(b) are in very good agreement with the experimental data of all considered oxygen isotopes $^{18-28}$O. The computed results by the MSDI interaction (green triangles in Figure-4(c)) are in poor agreement with the experimental data while those computed by the KUOSD interaction (red squares in Figure- 4(c)) are in agreement with the data at $18 \leq A \leq 21$ and in disagreement with the data at $22 \leq A \leq 28$. Inspection to Figure-4 shows that the calculated ground state binding energies with our I_2 interaction, which are very close to those of empirical interactions of USDB and WPN, are better describing the data of all considered oxygen isotopes than those of MSDI and KUOSD. It is important to point out that empirical interactions provide results are in better agreement with experiment than ours or anybody else.

Energy spectra of neutron rich $^{18\text{-}27}$O isotopes accomplished by our interactions (I_1 and I_2), empirical interactions (USDB and WPN) and theoretical interactions (MSDI and KUOSD) are displayed and compared with experiment in Figure-4.

Figure-5 demonstrates the low-lying energy spectrum of ^{18}O. Here, the ordering of the experimental $2_1^+, 4_1^+, 0_2^+$ and 2_2^+ excited states is properly predicted by I_1, I_2, MSDI and WPN interactions, where the excited state 0_2^+ is not seen in the MSDI spectrum because it lies above the 6 MeV. The ordering of the experimental 2_1^+ and 4_1^+ (0_2^+ and 2_2^+) excited states is correctly reproduced (reversed) by USDB and KUOSD interactions. This figure shows that the spectrum evaluated by I_1 is compressed compared with

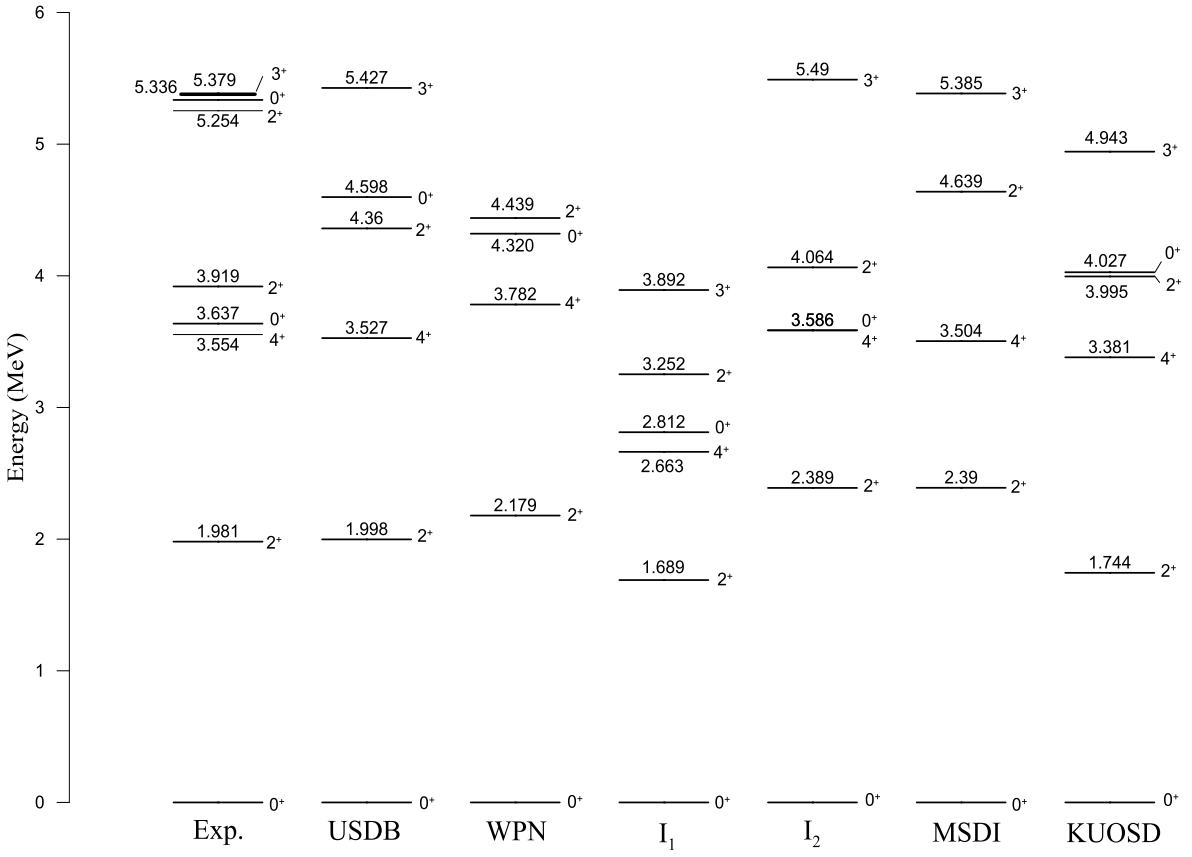

Figure 5- Comparison between experimental low lying energy spectrum of ^{18}O and those calculated with our I_1 and I_2 interactions, empirical USDB and WPN interactions, and theoretical MSDI and KUOSD interactions. The experimental data are taken from [22].

that of I_2 and experiment. The experimental excitation energies of 2_1^+ (1.981 MeV) and 4_1^+ (3.554 MeV) are very well characterized by USDB, slightly underestimated by KUOSD and slightly overestimated by WPN. For I_2 and MSDI, the calculated excitation energies of 2_1^+ are higher than the experimental value by about 0.409 MeV while those of 4_1^+ are in astonishing agreement with the experiment. The experimental excitation energy of 0_2^+ (3.637 MeV) is very well predicted by I_2 and over predicted by the rest of interactions whereas that of 2_2^+ (3.919 MeV) is very good explained by I2 and KUOSD and over predicted by USDB, WPN and MSDI. The experimental excitation energy of 3_1^+ (5.379 MeV), which is not shown in the spectrum WPN, is very well described by I_2, USDB and MSDI while in KUOSD is reasonably described.

Figure-6 displays the low-lying energy spectrum of ^{19}O. In this figure, the sequence of experimental excited states is suitably predicted by I_1 but the state $5/2_2^+$, which lies at 1.634 MeV, is too low compared with experiment (3.154 MeV). The sequence of observed states is appropriately conjectured by I_2, USDB and WPN interactions with the exception that the state $5/2_2^+$ is reversed with the state $3/2_2^+$. The sequence of experimental states is correctly (not correctly) reproduced by MSDI (KUOSD) interaction. Again, the spectrum formed with I_1 is compressed compared with that of I_2 and experiment. In the case of I_2 and MSDI, the states $3/2_1^+$ are considerably over predicted and the states $1/2_1^+$ are reasonably under predicted

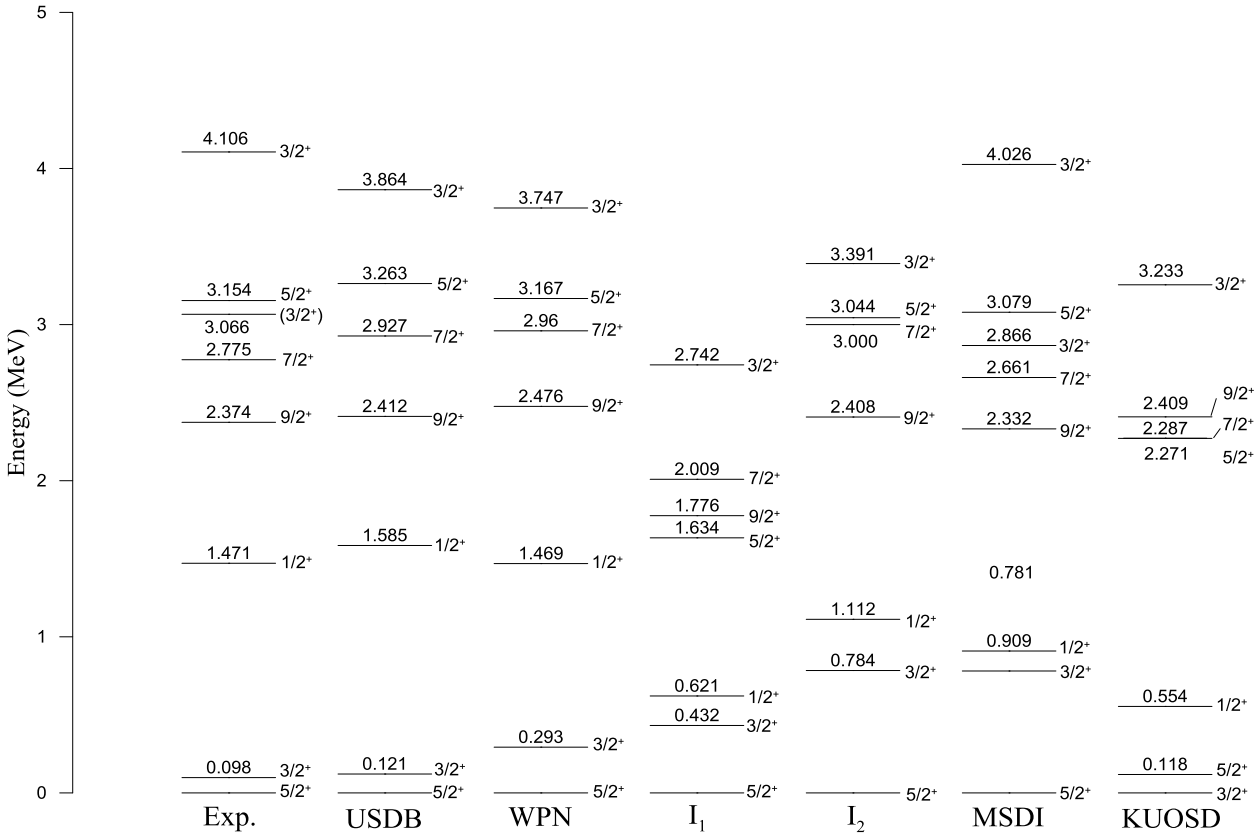

Figure 6- Same as in Figure-5 but for ^{19}O. The experimental data are taken from [25].

while the other states, which are above 2.3 MeV, are in very good agreement with experiment. Excitation energies calculated by USDB and WPN interactions are in good agreement with experiment. Excitation energies obtained by KUOSD are in poor agreement with experiment. Besides, the ground state binding energy evaluated with KUOSD is found to be $3/2_1^+$ instead of $5/2_1^+$, in disagreement with experiment.

Figure-7 reveals the low-lying energy spectrum of ^{20}O. The interactions of I_2, USDB and WPN suitably expect the sequence of the first three excited states ($2_1^+, 4_1^+$ and 2_2^+) and reverse it for the states 4_2^+ and 2_3^+. The interaction of MSDI rightly forecasts the sequence of the low lying energy spectrum and reverse it for the states 4_1^+ and 2_2^+. It is noticeable that both I_1 and KUOSD interactions do not truly predict the sequence of the low lying states, i.e. they reverse the sequence for the states 2_2^+ and 4_1^+ and also reverse it for the states 2_3^+ and 4_2^+. In general, the excitation energies calculated by USDB and WPN interactions are in a satisfactory description with those of experimental data while those calculated by I_2, MSDI interaction are in reasonable agreement with the data. For the spectra produced by I_1 and KUOSD interactions, the states are bunched above 2 and 3 MeV, respectively but the excitation energy of the 2_1^+ states are in agreement with experiment.

Figure-8 shows the low-lying energy spectrum of ^{21}O. In this figure, the sequence of states is correctly reproduced by I_1. The sequence of states is also rightly conjectured by I_2, USDB and WPN interactions with the exception that the state $7/2_1^+$ is reversed with the state $5/2_2^+$. The series of states obtained by MSDI interaction is analogous to those obtained by USDB and WPN interactions with the exception that

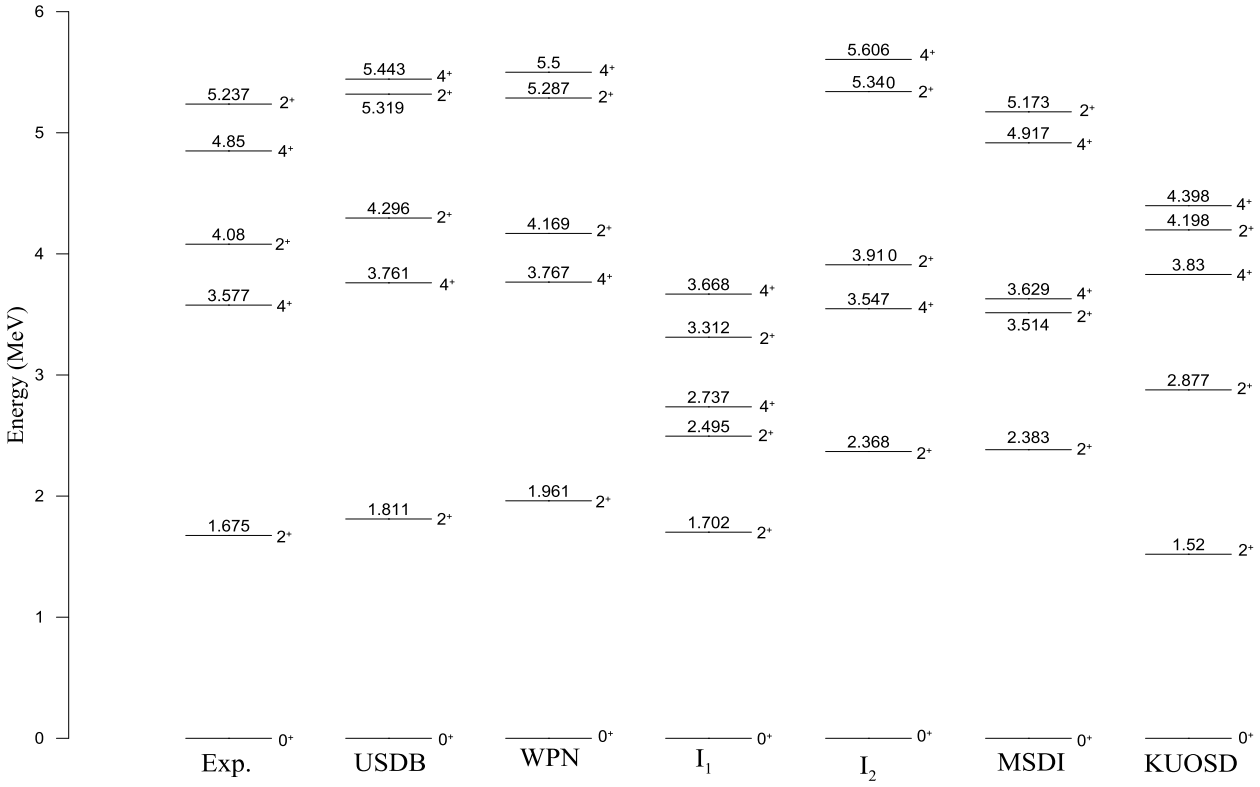

Figure 7- Same as in Figure-5 but for ^{20}O. The experimental data are taken from [23].

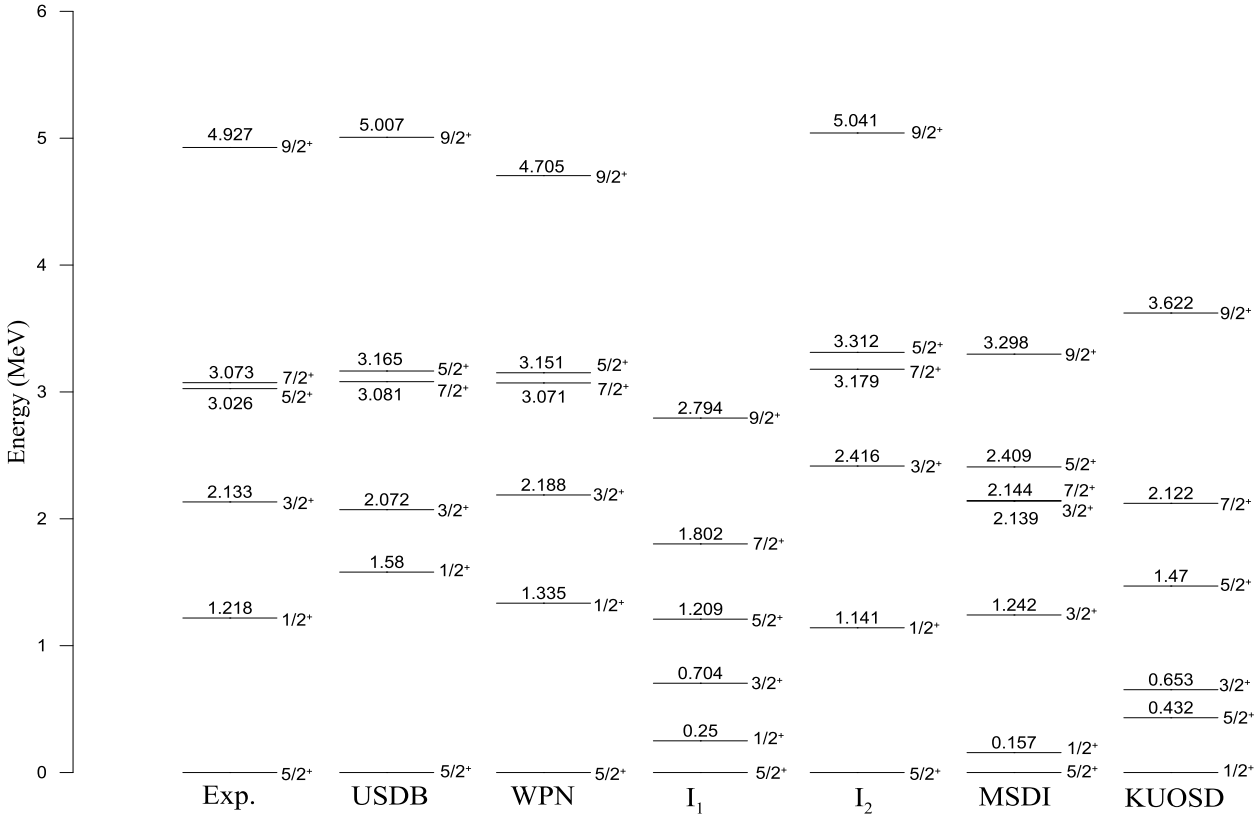

Figure 8- Same as in Figure-5 but for ^{21}O. The experimental data are taken from [23].

the state $3/2_2^+$ is seen at 2.139 MeV, which is slightly below to the state $7/2_1^+$. The sequence of states obtained by KUOSD interaction is also correctly reproduced with the exception that the ground

state is $1/2_1^+$ instead of the state $5/2_1^+$. The experimental excitation energies are very well forecasted by I_2, USDB and WPN interactions and under predicted by both the MSDI and KUOSD interactions. The spectrum obtained by I_1 is compacted compared to I_2 and experiment.

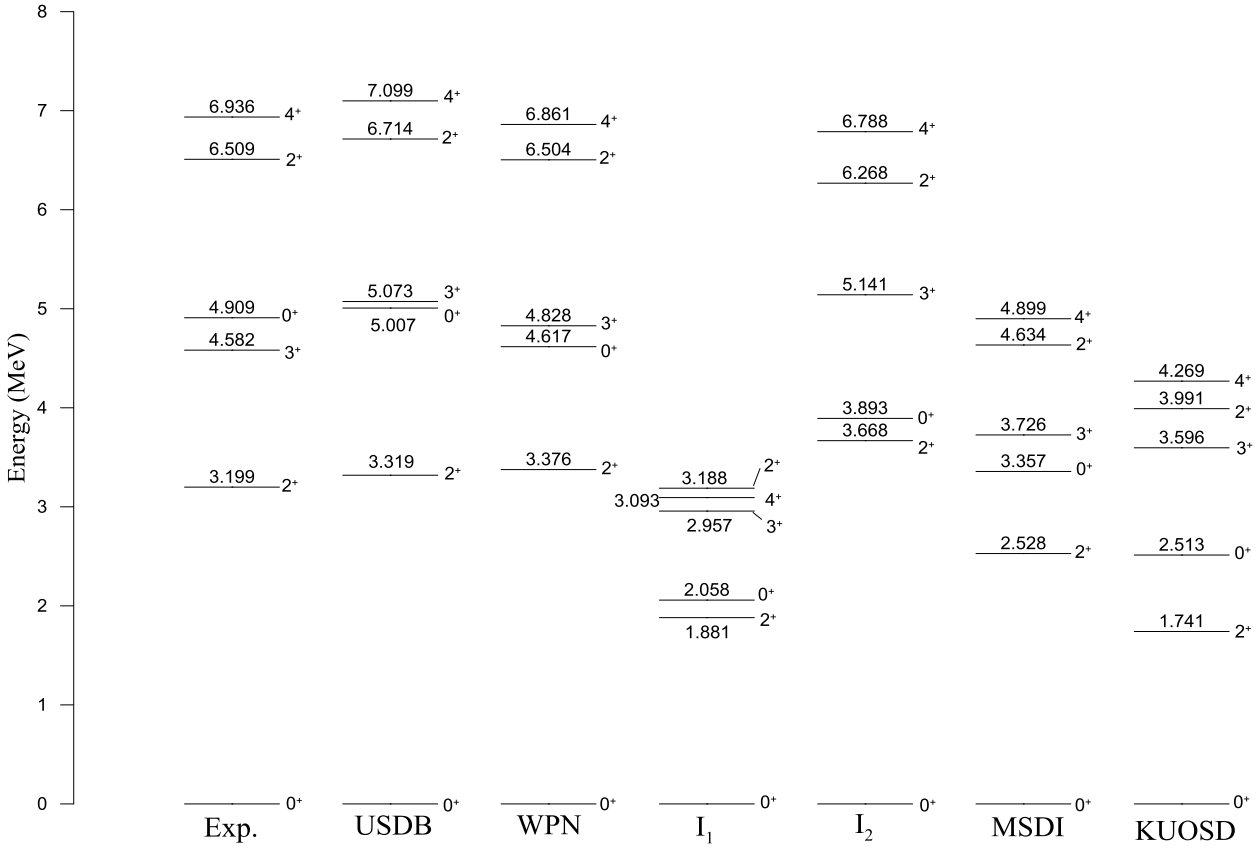

Figure 9- Same as in Figure-5 but for ^{22}O. The experimental data are taken from [23].

Figure-9 presents the low-lying energy spectrum of ^{22}O. Here, the ordering of energy levels is appropriately predicted by I_2, USDB, WPN, MSDI and KUOSD interactions with the exception that the level 0_2^+ is seen in place of the level 3_1^+. In the case of I_1 interaction, the ordering of levels is not correctly predicted because the level 0_2^+ (2_2^+) is reversed with the level 3_1^+ (4_1^+). Excitation energies evaluated by I_2, USDB and WPN interactions agree well with experiment but the WPN interaction gives more exact result for the excitation energies than I_2 and USDB or the other interactions. For the spectra formed by I_1, MSDI and KUOSD interactions, the energy levels are too compressed compared with experiment.

Figure-10 exhibits the low-lying energy spectrum of ^{23}O. It is clear the assembling of the observed low lying states is accurately foreseen via all considered interactions. The observed energy level of $5/2_1^+$ (2.70 MeV) is very well predicted by I_2, USDB and WPN interactions and considerably underestimated by I_1, MSDI and KUOSD interactions. The observed energy level of $3/2_1^+$ (4.00 MeV) is quite well predicted by USDB interaction, underestimated by WPN, KUOSD, I_1 and I_2 interactions, and considerably underestimated by MSDI interaction. However, the observed low lying energy spectrum of

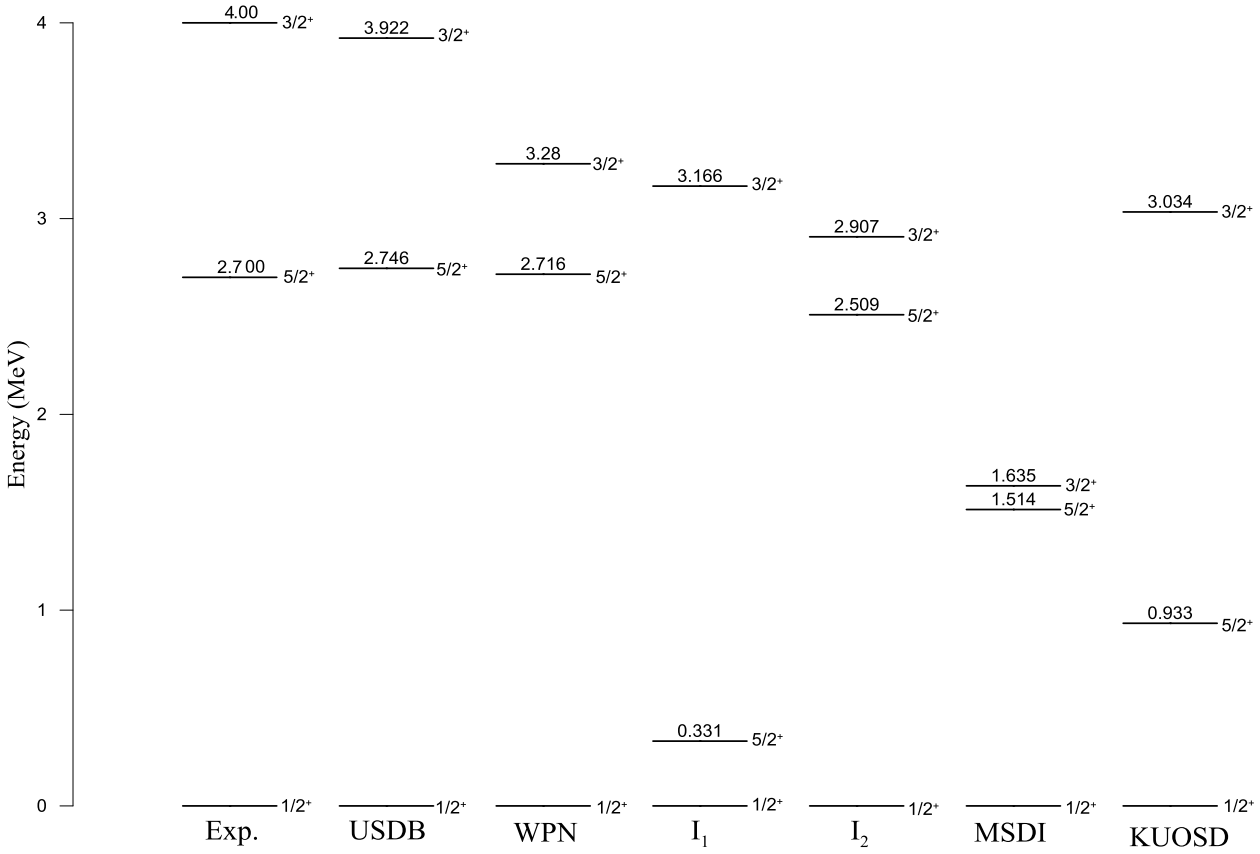

Figure 10- Same as in Figure-5 but for ^{23}O. The experimental data are taken from [26] and [27].

^{23}O is very well described by USDB and reasonably characterized by WPN, KUOSD, I_1 and I_2 interactions. In the case of MSDI interaction, the energy levels are bunched compared with those of observed data.

Figure-11 exposes the low-lying energy spectrum of ^{24}O. Here, the sequence of the observed low lying states is precisely predicted in terms of I1, USDB, WPN, MSDI and KUOSD interactions. In the case of I_2 interaction, the sequence of observed states is also correctly predicted but the state 0_2^+ comes in between the states 2_1^+ and 1_1^+. The observed excited state of 2_1^+ (4.790 MeV) is well predicted by I_1, I_2, USDB and KUOSD interactions, reasonably under predicted by WPN interaction and noticeably under predicted by MSDI interaction. The observed excited state of 1_1^+ (5.370 MeV) is very good predicted by I_1, I_2, WPN and KUOSD interactions, reasonably over predicted by USDB interaction and noticeably under predicted by MSDI interaction. The observed energy spectrum of ^{24}O is well explained by I_1, I_2, KUOSD, USDB and WPN interactions and not well explained by MSDI interaction. In this figure, the spins and parity in ^{24}O of a number of excited states around 7.5 MeV are predicted by I_1, I_2, USDB, WPN, MSDI and KUOSD interactions and accordingly shed light on the experiment [7].

Figure-12 exemplifies the low-lying energy spectrum of ^{25}O. In this figure, similar ordering of levels is found between the spectra of USDB and WPN interactions as well as among the spectra of I_1, I_2, MSDI and KUOSD interactions. It is noticed that the low-lying energy spectrum obtained via USDB interaction is higher, by an energy shift of about 0.8 MeV, than that of WPN interaction. Energy levels of MSDI are
more compressed while those of KUOSD are more spread and thus become closer in magnitude to those of USDB. Excitation energies obtained by I_2 are very close in magnitude to those of WPN. Energy levels above the state $1/2_1^+$ in I_1 interaction are very close in magnitude to those of USDB.

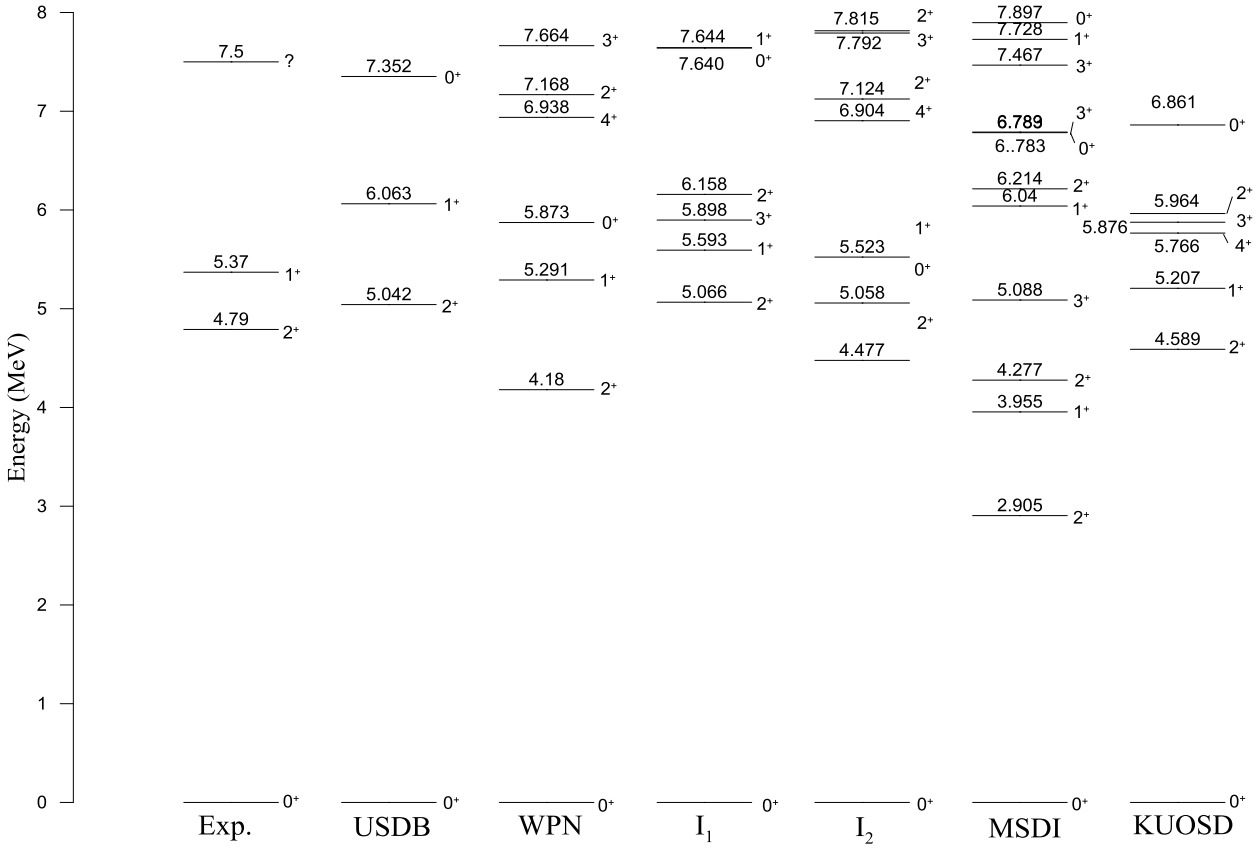

Figure 11- Same as in Figure-5 but for ^{24}O. The experimental data are taken from [3] and [7].

Figure-13 illustrates the low-lying energy spectrum of ^{26}O. The experimental sequence of low lying states is correctly predicted by all considered interactions. The newly observed excitation energy of 2_1^+ $(1.28^{+0.11}_{-0.08}$ MeV) [24] is very well predicted by I_1 (1.163 MeV) and over predicted by the rest of considered interactions. The interactions of I_1, I_2 and WPN give nearly similar excitation energy for the 2_2^+ state. Also, the interactions of USDB and KUOSD provide approximately the same values of excitation energy for the 2_2^+ state.

Figure-14 shows the low-lying energy spectrum of ^{27}O. In this figure, similar ordering of energy levels is obtained by all considered interactions. It is seen that the low-lying energy spectrum established by USDB interaction is higher, by an energy shift of about 0.85 MeV, than that of WPN interaction. As the energy levels of MSDI are compressed, we see those of KUOSD are more spread and then nearer in magnitude to those of I_1 interaction. Moreover, the spectrum produced by I_2 is very close to that obtained by WPN.

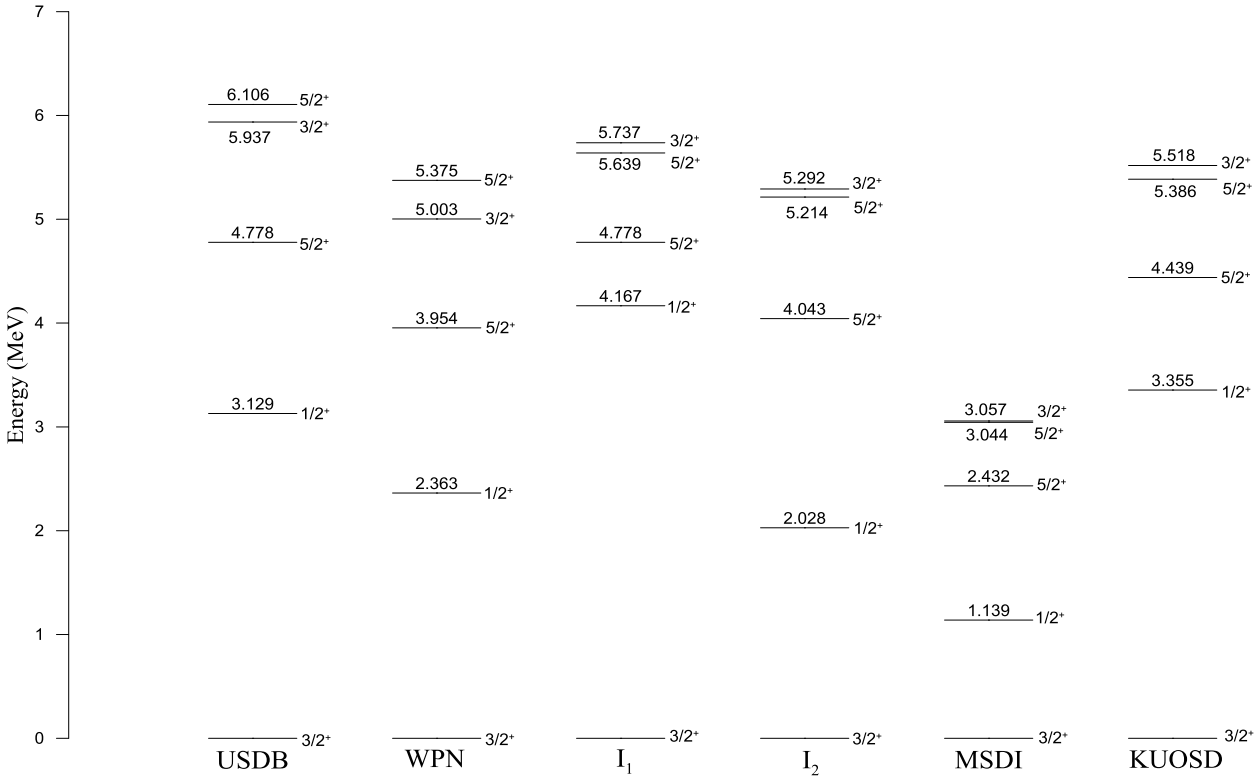

Figure 12- Same as in Figure-5 but for ^{25}O.

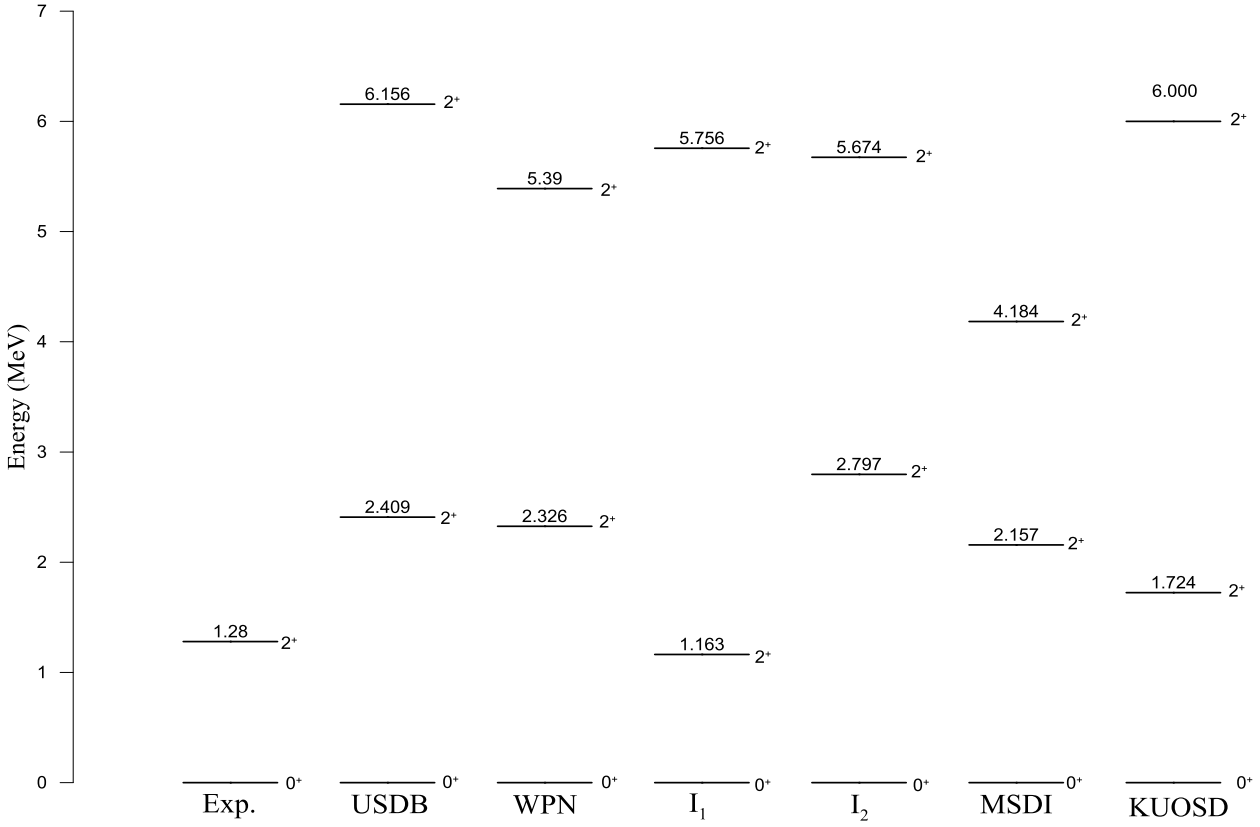

Figure 13- Same as in Figure-5 but for ^{26}O. The experimental data are taken from [24].

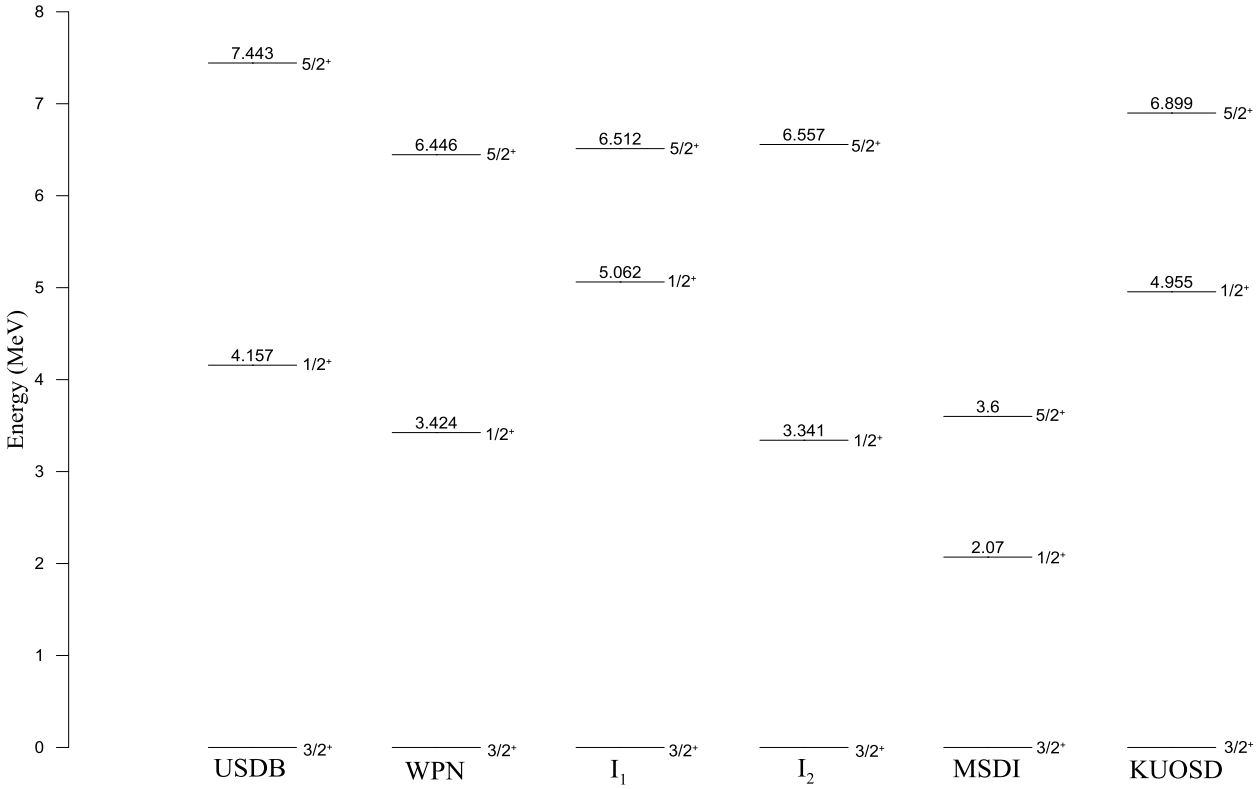

Figure 14- Same as in Figure-5 but for ^{27}O.

Conclusions

Generally, our modified interaction predicts well the ordering of levels, ground state binding energies and low lying energy spectra for all oxygen $^{18\text{-}28}$O isotopes. Our modified interaction confirms the location of the neutron drip line at $N = 16$ and also identifies the presence of the shell gap at $N = 14$ and $N = 16$, which proves the doubly magic behavior of ^{22}O and ^{24}O. Additionally, it predicts ^{26}O to be bound (in disagreement with experiment) and ^{28}O to be unbound (in agreement with experiment). It is noticed that the calculated results gained with our modified interaction, which are very close to those gained with the USDB and WPN interaction, are better than those gained with MSDI and KUOSD interactions.

Acknowledgement

The authors would like to express their thanks to Professor B. A. Brown of National Super-conducting Cyclotron Laboratory, Micihigan State University, for providing the computer code OXBASH.

References

1. Brown B. A. **2001**. The nuclear shell model towards the drip lines. *Progress in Particle and Nuclear Physics*, 47, pp:517-599
2. Thirolf P. G., Pritychenko B. V., Brown B. A., Cottle B. A., Chromik M., lasmacher T., Hackman G., Ibbotson R. W., Kempe K. W., Otsuka T., Riley L.A. and Scheit H. **2000**. Spectroscopy of the 2_1^+state in ^{22}O and shell structure near the neutron drip line. *Physics. Letters B*, 485, pp:16-22
3. Hoffman C. R., Baumann T., Bazin D., Brown J., Christian G., Denby D.H., DeYoung P. A., Finck J. E., Frank N., Hinnefeld J., Mosby S., Peters W. A., Rogers W. F., Schiller A., Spyrou A., Scott M. J., Tabor S. L., Thoennessen M., and Voss P. **2009**. Evidence for a doubly magic ^{24}O. *Physics Letters B*, 672, pp: 17-21.
4. Kanungo R., Nociforo C., Prochazka A., Aumann T., Boutin D., Cortina-Gil D., Davids B, Diakaki M, Farinon F., Geissel H., Gernhauser R., Gerl J., Janik R., Jonson B., Kindler B., Knobel R., Krucken R., Lantz M., Lenske H., Litvinov Y., Lommel B., Mahata K., Maierbeck P.,

Musumarra A., Nilsson T., Otsuka T., Perro C., Scheidenberger C., Sitar B., Strmen P., Sun B., Szarka I., Tanihata I., Utsuno Y., Weick H. and Winkler M. **2009**. One-neutron removal measurement reveals ^{24}O as a new doubly magic nucleus. *Physical Review Letters*, 102, pp: 152501(1-4).

5. Hoffman C. R., Baumann T., Bazin D., Brown J., Christian G., DeYoung P. A., Finck J. E., Frank N., Hinnefeld J., Howes R., Mears P., Mosby E., Mosby S., Reith J., Rizzo B., Rogers W. F., Peaslee G., Peters W. A., Schiller A., Scott M. J., Tabor S. L., Thoennessen M., Voss P. J., and Williams T. **2008**. Determination of the N =16 shell closure at the oxygen drip line. *Physical Review Letters*, 100, pp: 152502(1-5).

6. Lunderberg E., DeYoung P. A., Kohley Z., Attanayake H., Baumann T., Bazin D., Christian G., Divaratne D., Grimes S. M., Haagsma A., Finck J. E., Frank N., Luther B., Mosby S., Nagi T., Peaslee G. F., Schiller A., Snyder J., Spyrou A., Strongman M. J., and Thoennessen M. **2012**. Evidence for the Ground-State Resonance of ^{26}O. *Physical Review Letters*, 108, pp: 142503(1-5).

7. Hoffman C. R., Baumann T., Brown J., DeYoung P. A., Finck J. E., Frank N., Hinnefeld J. D., Mosby S., Peters W. A., Rogers W. F., Schiller A., Snyder J., Spyrou A., Tabor S. L., and Thoennessen M. **2011**. Observation of a two-neutron cascade from a resonance in ^{24}O. *Physical Reviw C*, 83, pp: 031303(R) (1-5).

8. Volya A. and Zelevinsky V. **2005**. Discrete and Continuum Spectra in the Unified Shell Model Approach. *Physical Review Letters*, 94, pp: 052501(1-4).

9. Hagen G., Papenbrock T., Dean D. J., Hjorth-Jensen M., and Velamur Asokan B. **2009**. *Ab initio* computation of neutron-rich oxygen isotopes. *Physical Review C*, 80, pp: 021306 (R) (1-5).

10. Otsuka T., Suzuki T., Holt J. D., Schwenk A., and Akaishi Y. **2010**. Three-body forces and the limit of oxygen isotopes. *Physical Review Letters* 105, pp: 032501(1-4).

11. Entem D. R. and Machleidt R. **2003**. Accurate charge-dependent nucleon-nucleon potential at fourth order of chiral perturbation theory. Physical Review C, 68, pp: 041001(R) (1-5).

12. Fiase J., Hamoudi A., Irvine J. M. and Yazici F. **1988**. Effective interactions for sd-shell-model calculations. *Journal of Physics G: Nuclear Physics*, 14, pp: 27-36.

13. Reid R. V. **1968**. Local phenomenological nucleon-nucleon potentials. *Annals of Physics*, 50, pp: 411-448.

14. Wildenthal B. H. **1984**. Empirical strengths of spin operator in nuclei. *Progress in Particle and Nuclear Physics*, 1, pp: 5-51.

15. Brown B. A. and Richter W. A. **2006**. New USD Hamiltonians for the sd-shell. *Physical Review C*, 74, pp: 034315(1-11).

16. Irvine J. M. **1981**. Constrained variational calculations for the nuclear many-body problem. *Progress in Particle and Nuclear Physics*, 5, pp: 1-54.

17. Irvine J. M., Mani G. S., Pucknell V. F. E., Vallieres M. and Yazici F. **1976**. Nuclear shell model calculations and strong two-body correlations. *Annals of Physics*, 102, pp: 129-155.

18. Brown B. A., Etchegoyen A., Godin N. S., Rae W. D. M., Richter W. A., Ormand W. E., Warburton E. K., Winfield J. S., Zhao L. and Zimmermam C. H. **1984**. The computer code oxbash. *MSU-NSCL Report Number 524*.

19. Audi G., Wapstra A. H. and Thibault C. **2003**. The AME2003 atomic mass evaluation. *Nuclear Physics A*, 729, pp: 337-676.

20. Wildenthal B. H. and Mcgrory J. B. **1971**. Structure of nuclei with masses A = 30-35 as calculated in the shell model. *Physical Review C*, 4(5),pp: 1708-1758.

21. Kuo T. T. S. **1967**. State dependence of shell-model reaction matrix elements. *Nuclear Physics A*, 103, pp: 71-96.

22. Oertzen W. von, Dorsch T., Bohlen H .G., Krucken R., Faestermann T., Hertenberger R., Kokalova Tz., Mahgoub M., Milin M., Wheldon C., and Wirth H. F. **2010**. Molecular and cluster structures in ^{18}O. *The European Physical journal A*, 43, pp: 17-33.

23. Stanoiu M., Azaiez F., Dombrádi Zs., Sorlin O., Brown B. A., Belleguic M., Sohler D., Saint Laurent M. G., Lopez-Jimenez M. J., Penionzhkevich Y. E., Sletten G., Achouri N. L., Angélique J. C., Becker F., Borcea C., Bourgeois C., Bracco A., Daugas J. M., Dlouhý Z., Donzaud C., Duprat J., Fülöp Zs., Guillemaud-Mueller D., Grévy S., Ibrahim F., Kerek A., Krasznahorkay A., Lewitowicz M., Leenhardt S., Lukyanov S., Mayet P., Mandal S., van der Marel H., Mittig W., Mrázek J., Negoita F., De Oliveira-Santos F., Podolyák Zs., Pougheon F., Porquet M. G.,

Roussel-Chomaz P., Savajols H., Sobolev Y., Stodel C., Timár J., and Yamamoto A. **2004**. *N*=14 and 16 shell gaps in neutron-rich oxygen isotopes. *Physical Review C*, 69, pp: 034312(1-10).

24. Kondo Y., Nakamura T., Tanaka R., Minakata R., Ogoshi S., Orr N. A., Achouri N. L., Aumann T., Baba H., Delaunay F., Doornenbal P., Fukuda N., Gibelin J., Hwang J.W., Inabe N., Isobe T., Kameda D., Kanno D., Kim S., Kobayashi N., Kobayashi T., Kubo T., Leblond S., Lee J., Marqués F. M., Motobayashi T., Murai D., Murakami T., Muto K., Nakashima T., Nakatsuka N., Navin A., Nishi S., Otsu H., Sato H., Satou Y., Shimizu Y., Suzuki H.,Takahashi K., Takeda H.,Takeuchi S., Togano Y., Tuff A. G., Vandebrouck M. and Yoneda K. **2016**. Nucleus ^{26}O: A barely unbound system beyond the drip line. *Physical Review Letters*, 116, pp: 102503(1-6).

25. Oertzen W. von, Milin M., Dorsch T., Bohlen H.G., Krucken R., Faestermann T., Hertenberger R., Kokalova Tz., Mahgoub M., Wheldon C., and Wirth H. F. **2010**. Shell model and band structures in ^{19}O. *The European Physical Journal A*, 46, pp: 345-358.

26. Elekes Z., Dombra´di Zs., Aoi N., Bishop S., Fulop Zs., Gibelin J., Gomi T., Hashimoto Y., Imai N., Iwasa N., Iwasaki H., Kalinka G., Kondo Y., Korsheninnikov A. A., Kurita K., Kurokawa M., Matsui N., Motobayashi T., Nakamura T., Nakao T., Nikolskii E.Yu., Ohnishi T. K., Okumura T., Ota S., Perera A., Saito A., Sakurai H., Satou Y., Sohler D., Sumikama T., Suzuki D., Suzuki M., Takeda H., Takeuchi S., Togano Y., and Yanagisawa Y. **2007**. Spectroscopic Study of Neutron Shell Closures via Nucleon Transfer in the Near-Dripline Nucleus ^{23}O. *Physical Review Letters*, 98, pp: 102502(1-4).

27. Schiller A., Frank N., Baumann T., Bazin D., Brown B. A., Brown J., DeYoung P. A., Finck J. E., Gade A., Hinnefeld J., Howes R., Lecouey J.-L., Luther B., Peters W. A., Scheit H., Thoennessen M., and Tostevin J. A. **2007**. Selective population and neutron decay of an excited state of ^{23}O. *Physical Review Letters*, 99, pp: 112501(1-4).